ORIGINAL PAPER

Design of highly porous melamine-based networks through a bicontinuous microemulsion templating strategy

C. C. Egger · C. du Fresne · D. Schmidt ·
J. Yang · V. Schädler

Abstract Designing low density polymeric porous materials with defined pore sizes (diameters in the 100 nm range) still remains a real synthesis challenge. Here, for the first time, we present a strategy by which bicontinuous microemulsions are used as templating agents for the in-situ aqueous polycondensation of organic resins (melamine formaldehyde, MF). The behaviour of surfactants with different head-groups in systems including oil and MF-containing aqueous phase is studied. While many surfactants are not compatible with aqueous MF precondensates, here we report a non-ionic surfactant either used solely or along with anionic surfactants which prove to be successful at keeping bicontinuous microemulsion systems homogeneous even during early stages of polymerisation. However, upon acid-catalysis it becomes clear that the pore structure of the organic material is largely controlled by the kinetics of phase separation due to the sol–gel process rather than by the thermodynamic equilibrium of the template (microemulsion). Indeed, despite numerous attempts, stabilising the microemulsion interface with zero curvature (bicontinuous) has remained problematic. Instead, we show a new behaviour for the MF resin whereby non-spherical MF morphologies (i.e. thread-like structures) can be obtained by specific interactions between the aqueous amino resin and the acid counterions.

C. C. Egger (✉)
Lennard Jones Laboratories, Keele University, Keele,
Staffordshire ST5 5BG, UK
e-mail: c.c.egger@chem.keele.ac.uk

C. du Fresne
BASF Nederland B.V. Innovatielaan 1, 8466 SN Nijehaske,
The Netherlands

D. Schmidt
Department of Plastics Engineering, University of Massachusetts
Lowell, Lowell, MA, USA

J. Yang
BASF China, 20/F, Harbour Ring Plaza,
Shanghai 200001, China

V. Schädler
BASF Corporation, 1609 Biddle Avenue, Wyandotte,
MI 48192, USA

1 Introduction

The era of porous materials in chemistry may have begun in the late XVIIIth century when Cronstedt discovered the existence of zeolite minerals on Earth and the presence of pores in which water was entrapped [1]. From then, along with the new tools available to the chemists, a range of porous materials has been prepared synthetically [2, 3]. Such networks have well defined pore size, pore volume, morphology for given application (e.g. catalysts, molecular sieves, chromatographic columns, sensors). The precise design of pore size can follow different routes summarised in Fig. 1. The pores are either (i) pre-defined in the structure through the use of templates which are temporarily present to induce controlled precipitation of a matrix and/or used as porogens only—advent of the MCM-type materials in 1991–1992 [4, 5], (ii) formed by controlled phase separation of a growing polymer in its solvent with subsequent
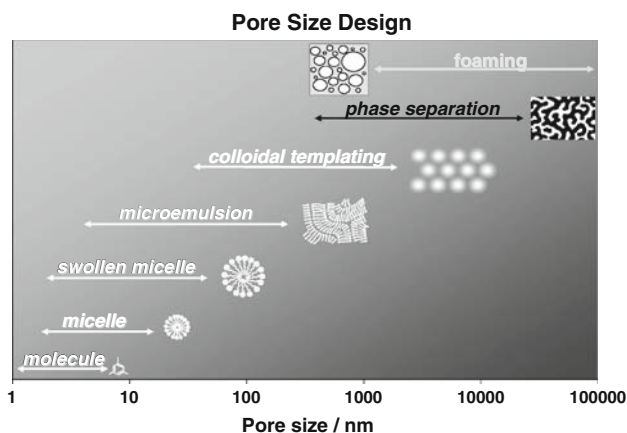
Pore Size Design

Fig. 1 Schematic representation of the various strategies used to design pores in a given matrix: (i) the templating approach by which *molecules*, *micelles*, *microemulsions*, *colloids* are used to create the cavity, (ii) the sol–gel approach by which the *phase separation* between the growing polymer and the solvent is controlled, (iii) the physical approach by which bubbles of gas are intruded in a matrix (*foaming*)

drying of the solvent—the aerogel materials [6], (iii) "injected" through gas bubbles in a melt which is further solidified—macroscopic foams. Average diameters vary greatly with synthesis strategy and tend to range from a few Angstroms for path (i) to tens of microns for method (iii). Yet, for all routes, they are numerous specimens now commercially available. However, designing porous networks remains incredibly challenging when tackling *very low density materials* (<150 g/L) with *small pores diameters* (<200 nm). Indeed, even if the space for void is technically created through one of the three approaches described above, it is only truly generated upon removing the template or solvent. This drying step can be particularly difficult to apply successfully as strong capillary pressures are engendered within the pores. Indeed, according to the Young Laplace equation, applied to the specific case of a spherical interface:
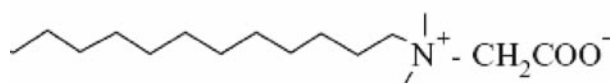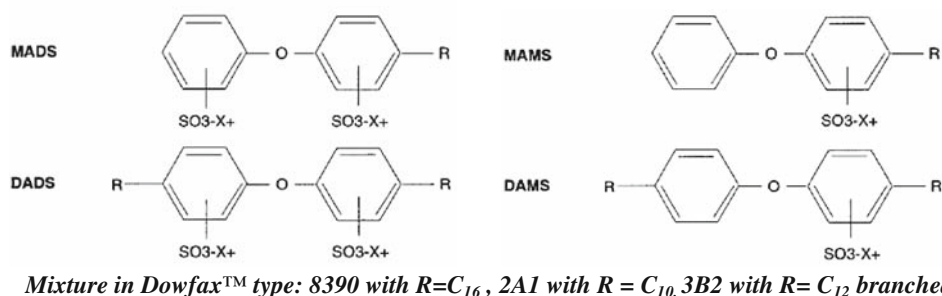
$$P_c = \frac{2\sigma}{r}$$

r (m) = radius of capillary, σ (mN/m) = liquid surface tension, the capillary pressure P_c is a function of the surface tension of the solvent to dry out, and the radius of the pore in which the solvent lies. When the pore size goes down to ∼100 nm, P_c can be as high as 1.5×10^6 Pa, which is 15 times higher than the atmospheric pressure (1×10^5 Pa). These high pressures can have dramatic effects on the structure and can cause it to collapse. Moreover, if the network is rendered more fragile by increasing the density of the pores in the matrix, it will certainly collapse upon drying. If the framework is robust

enough to sustain the capillary pressures then highly porous materials with small pores result. This is the case with ceramic foams. Another way around the loss of porosity through structural collapse is the careful control of the drying process. Typically, aerogels are formed by placing them in a solvent (CO_2) that is then removed under supercritical conditions, so that the surface tension of the fluid vanishes (see Laplace equation above). As for the foaming process although it does not require the removal of a solvent/template, it has proved difficult to increase the pore density and diminish the pore size [7, 8].

In order to design a nanoporous organic material of rather low density, we demonstrate here a strategy that relies on a bicontinuous microemulsion as a template. This technique was chosen as it allows designing light structures in the range between 10 and 100 nm which is interesting for an industrial application such as separation. Microemulsions are thermodynamically stable mixtures of water and oil stabilised at the interface with surfactant molecules. Under the appropriate conditions (temperature, salt, composition) bicontinuous structures can be formed. For such systems, an interpenetrating three-dimensional network of oil and water coexist either through a three-phase region (with an excess of oil and water) or a one-phase region (no excess). These thermodynamically stable domains have dimensions in the range of a few tens of nanometers as described elsewhere [9, 10] and consequently can template the formation of nanoporous materials. The approach by itself is not new but has been restricted up to now to systems involving radical polymerisation [11, 12]. To our knowledge this is the first time that the combination of microemulsion templating and polycondensation of an organic monomer in an aqueous phase is reported. The strategy involves the use of soluble monomers in the water phase such as melamine formaldehyde (MF) which are allowed to polycondense under acid-catalysis around the oil moiety potentially retaining the template structure.

Figure 2 represents a quaternary phase diagram of a surfactant in oil and water with varying temperature (left) and a binary phase diagram of a non-ionic surfactant also referred to as "Fish" diagram for which oil and water is fixed (right). Understanding surfactant behaviour in water requires dedicated studies and it is even more true for microemulsions. The objective of this work being to assess whether new nanoporous materials with very low densities can be chemically constructed, the work has focussed on the polycondensation side and has essentially relied on relevant literature about behaviour of surfactants in microemulsions systems [13–15]. When novel surfactants are tried in oil and water, then the behaviour is only checked visually in a series of vials with varying surfactant concentrations: appearance of a bluish colour typical of a

Fig. 2 *Left*: Quaternary phase diagram of a surfactant in various oil-to-water ratios with varying temperature. *Right*: Schematic binary phase diagram ("Fish diagram") of a non-ionic surfactant for a given oil-to-water composition, showing the evolution from a two-phase region (oil-in-water or water-in-oil) or a three-phase region (bicontinuous region with excess water and oil) towards a one-phase region (bicontinuous microemulsion = 3D nanoscopic network) with increasing surfactant concentration

bicontinuous network due to Rayleigh scattering and temperature inversion for which the microemulsion goes from an oil-in-water to a water-in-oil phase (or vice-versa for an ionic head-group). In order to tune the efficiency of surfactant molecules at designing melamine-formaldehyde containing bicontinuous microemulsions, mixtures using four types of surfactants are utilised: purely non-ionic, purely anionic, gemini or zwitterionic and finally mixture anionic/non-ionic. Indeed, ought to their charged head groups, ionic surfactants show phase diagrams greatly influenced by temperature and salinity, two parameters easily tunable experimentally. In general, an ionic surfactant can be tuned from hydrophobic to hydrophilic by raising the solution temperature. In presence of salt, the salt ions compete with the head groups and the counter-ions for water of hydration. As a consequence, electrostatic charges are screened on head-groups, rendering the surfactant molecules less polar so that they can stabilise water-in-oil microemulsions (the schematic "Fish" diagram displayed Fig. 2 is then inverted).

2 Experimental

2.1 Materials

Phase behaviours of the following surfactants are studied in pseudo-ternary systems with water (with or without salt), oil, and surfactant:

(1) Purely non-ionic systems: Lutensol[TM] TO7 (saturated iso-C13 alcohol BASF-AG, with 7 EO units 100% pure).

(2) Purely anionic systems: (i) AOT (Sulfosuccinic acid bis(2-ethylhexyl) ester sodium salt, Sigma-Aldrich product, 100% pure). (ii) Lutensit[TM] AEP (acid phosphoric ester of a fatty alcohol ethoxylate BASF-AG 100% pure). (iii) SDS, sodium dodecyl sulphate (Sigma Aldrich, 100%).

(3) Gemini or zwitterionic systems: Surfactants (Alkyldiphenyloxide disulphonate Dowfax[TM] 8390, 2A1 and 3B2 from DOW) with Butanol as a co-solvent, or Carboxybetaine (Lauryl betaine Amphoteen[TM] 24 Akzo Nobel).

(4) Mixed ionic–non-ionic systems: AEP or SDS are mixed in small proportions (never higher than 20 wt.% of the total amount of surfactant used) with a non-ionic surfactant (Lutensol[®] TO7).

Mixture in Dowfax™ type: 8390 with R=C$_{16}$, 2A1 with R = C$_{10,}$ 3B2 with R= C$_{12}$ branched

Lauryl betaine Amphoteen^{TM} 24

MF resins are BASF-AG products with M:F 1:1.5 or 1:3.6 molar ratio. Acid catalysts are purchased from Aldrich-Fluka: H$_3$PO$_4$ 85% from Aldrich, H$_2$SO$_4$ 100% from Aldrich HCl 37% from Aldrich, HCOOH 100% from Fluka.

2.2 Phase behaviour and polymerisation

Components are mixed in vials and placed in a water bath at 60 °C for 12 h for rapid diffusion and mixing, left to cool down to RT, and then heated up again to 70 °C, 5 °C/step, 12 h/step. This second heating ramp, much slower, allows for a good homogenisation of the ternary or quaternary mixtures throughout the entire volume, in order to reach at each temperature step a thermodynamic equilibrium for which a stable emulsion is obtained. Phase behaviour is checked visually for each step: number of phases, volume changes in the water or the oil phase, cloudiness. From these observations, a partial phase diagram can be drawn for a given oil/water ratio and as a function of temperature and surfactant concentration. Polymerisation of MF precondensates in the aqueous regions of bicontinuous microemulsions is carried out by replacing the water phase with a MF solution. The composition and nature of the other components (oil and surfactant) remain the same. The phase behaviour of the new pseudo-quaternary system is re-studied to allow for small variations due to the hydrophilicity of the MF. When the microemulsion including the monomer remains bicontinuous, fresh mixtures are prepared for which the catalyst is added. Vials are then heated at 60 °C in a water bath for an appropriate time (although gelation can occur very fast, for hardening purpose, gels are left at least 2 days at 60 °C). After the ageing process, gels are taken out and either dried under ambient conditions or solvent-exchanged twice with ethanol and pentane successively, before drying in air. Samples showing little shrinkage are characterised by SEM and mercury intrusion.

2.3 Mercury intrusion measurements

An AutoPore IV 9500 (Micromeritics USA, available at BASF-Aktiengesellschaft, Ludwigshafen) was employed with a logarithmic step scan mode between 0.003 and 400 MPa with equilibration times varying between 10 s (low pressure) and 20 s (high pressure).

2.4 Scanning electron microscopy (SEM)

In order to access the bulk of the materials, fractured specimens were mounted on a double-sided conducting carbon disc, stuck on a 235 mm flat stub and when required sputtered on an Emitech Sputterer type K575X at 60 mA for 20 s with a gold target. Depending on the vacuum quality, a uniform 10 to 20-nm coating was obtained. Samples were then imaged on a Dual Beam Strata 235 from FEI, with a 5 keV electron beam using spot size 3 (associated spot size 2.1 nm).

2.5 Porosity and density calculations from mercury data

The ratio of porous volume within the specimen is:

$$\%P_v^{Hg} = \left[\frac{V_i}{\left(\frac{1}{\rho_t}\right) + V_i} \right] \times 100$$

with V_i the volume intruded by mercury, and ρ_t the full density of MF, and the bulk density ρ_{calc} is:

$$\rho_{calc} = \frac{(100 - P_v) \times \rho_t}{100}$$

3 Results and discussion

The various types of surfactants used in this study in order to form bicontinuous microemulsions are displayed in Table 1 along with their temperature range and their sensitivity to brine content. The effect of the incorporation of the melamine formaldehyde and then the acid catalyst on the apparent homogeneity of the system is also indicated (For detail about starting compositions, see Table 2). Ought to the hydrophilic character of the MF resin, a perturbation in the hydrophobicity/hydrophilicity balance of the bicontinuous microemulsion is often observed upon addition of the monomer, and the three-dimensional network is no longer retained. Moreover, attempts to prepare microemulsions with gemini or zwitterionic surfactants along with the MF resin are all unsuccessful due to a real difficulty in homogeneously dissolving the precondensate MF resin (usually a precipitation is observed). Yet, a promising route arises with the succinic acid based anionic AOT surfactant, in which the bicontinuous structure of the microemulsion is not only retained in presence of MF but is also stable in time (>2 days). Unfortunately, as soon as the catalyst is added, a fast phase separation is always observed. Full polymerisation with no clear phase separation is only observed in the case of microemulsions made from purely non-ionic systems or from a mixture of non-ionic/ionic surfactants. Indeed, when the non-ionic surfactant C_{13} oxo alcohol ethoxylate Lutensol® TO7 is used to stabilise a microemulsion formed with a monomeric MF containing aqueous phase and pentane as the oil phase (or heptane), the bicontinuity of the microemulsion is retained as shown in Fig. 3, top left: the formed fluid is a one phase system with a characteristic blue tint. Upon acid-catalysis

Table 1 Various surfactant systems used in this work to prepare bicontinuous microemulsions

Surfactant type	Surfactant specimen	Microemulsion			Polymerisation	
		Efficiency	Temperature (°C)	Salinity	Stability with resin	Stability with catalyst
Non-ionic	Lutensol TO7	∼10%	55–65	Insensitive	Good	Good
Anionic	Lutensit AEP	∼10%	45–55	Sensitive	Precipitation	Precipitation
	AOT	∼8%	50–55	Sensitive	Good	Precipitation
	SDS	∼10%	40–65	Sensitive	Precipitation	Precipitation
Ionic/non-ionic	10–20 wt.% AEP (or SDS) in TO7	∼10%	55–70	Sensitive	Good	Good
Gemini	Dowfax 8390/2A1/3B2	∼10%	45–70	Sensitive	Precipitation	Precipitation
Zwiterionic	Amphoteen 24	∼6%	Insensitive	Insensitive	Precipitation	Precipitation

The temperature range for which a three- or one-phase region is observed is given, as well as the sensitivity towards salt ions. The stability of the given microemulsions as checked visually is given when the MF monomer is introduced and after acid-catalysis

Table 2 Chemical composition of the microemulsions μE-001 to μE-004 shown in this work: the oil-to-water ratio is kept constant to 0.5 in volume, the melamine-formaldehyde based resin has a concentration varying from 17 to 8 wt.%

Specimen	Melamine formaldehyde	Surfactant	Oil/water (volume)	Acid	Temperature (°C)
μE-001	(M:F 1:3.6 mol) 17 wt.%	Lutensol TO7[a], 8.3 wt.%	Heptane/water 0.50	H_3PO_4 (85%) 4.3 wt.%	64
μE-002	(M:F 1:1.5 mol) 11 wt.%	20 wt.% AEP[b] in TO7, Total 10 wt.%	Heptane/water 0.55	HCl (37%) 2.1 wt.%	60
μE-003	(M:F 1:1.5 mol) 8 wt.%	20 wt.% SDS[c] in TO7, Total 10 wt.%	Heptane/water 0.54	H_3PO_4 (85 wt.%) 2.1 wt.%	60
μE-004	(M:F 1:1.5 mol) 8 wt.%	10 wt.% SDS in TO7, Total 10 wt.%	Heptane/water 0.54	HCO_2H (100%) 2.5 wt.%	60
MF001	(M:F 1:1.5 mol) 11 wt.%	NA	NA	H_2SO_4 (85%) 4 wt.%	60
MF002	(M:F 1:1.5 mol) 11 wt.%	NA	NA	HCO_2H (100%) 4 wt.%	60

The overall surfactant content is kept around 10 wt.% and the acid amount varies from 2 to 4 wt.%. Microemulsions with both non-ionic and ionic surfactants are investigated using strong or weak acid catalysts. The chemical compositions of the two gels leading to the xerogels MF-001 and MF-002 are also given

[a] Lutensol-TO7 or TO7 is iC_{13}-$(EO)_7H$

[b] AEP or Lutensit-AEP is $iC_{13}(EO)_7PO_3H_2$

[c] SDS stands for Sodium Dodecyl Sulfate

with a strong acid, the MF-containing aqueous phase polymerises and a homogeneous gel is formed (see Fig. 3 top right) showing only a slight increase in turbidity compared to the unreacted microemulsion. Further insights into the resulting dry material labelled µE-001 are necessary to evaluate final porosity and pore size distribution. The SEM micrographs of µE-001 in Fig. 3 bottom clearly show the existence of droplet-like pores, regularly dispersed throughout the polymerised MF matrix, with no indication for a microemulsion-like intertwined three-dimensional network of voids and solid polymer on a 10–100 nm scale as would have been expected if the microemulsion had acted as a template. Mercury intrusion measurements also indicate large pores (average diameter: 1.2 µm) and small surface area (17 m^2/g). The calculated porosity reaches only 47 vol.%. Although on a macroscopic level the gel appears to be homogeneous, the microscopic investigation reveals that the pre-existing bicontinuous microemulsion structure could not be retained upon such acid-catalysis.

When 20 wt.% of the non-ionic surfactant is replaced with an anionic surfactant (AEP or SDS), bicontinuous microemulsions are still formed. Upon acid-catalysis and subsequent drying, materials µE-002 and µE-003,

respectively, are produced: µE-002 exhibits bimodal porosity with pore diameters in the range of 30 microns and 1 micron or less. Despite a low surface area (156 m^2/g) the porosity is high (89 vol.%) and is scattered irregularly throughout the matrix as shown by SEM in Fig. 4. µE-003 results in smaller pores (<2.3 microns) distributed more homogeneously within the MF matrix leading however to a denser material (73 vol.% porosity). In both cases addition of an ionic component could not prevent the nanoscopic microemulsion structure to collapse upon polymerisation of the monomeric MF precursor. Obviously, larger polymer aggregates are formed during condensation of the MF. Note that the monomeric MF precursor is perfectly soluble in water while the resulting MF network is completely insoluble under aqueous conditions. The phase separation of the MF polymer formed within the aqueous phase is driven by the increase in hydrophobicity when the methylol groups of the monomeric MF react to form ether or methylene bridges [16]. Above a given molecular weight and concentration of the MF species the latter phase separates from the aqueous domain of the microemulsion and forms larger aggregates in order to minimize the interfacial energy. At this point the polymer will disrupt the bicontinuous template to form large domains from which the
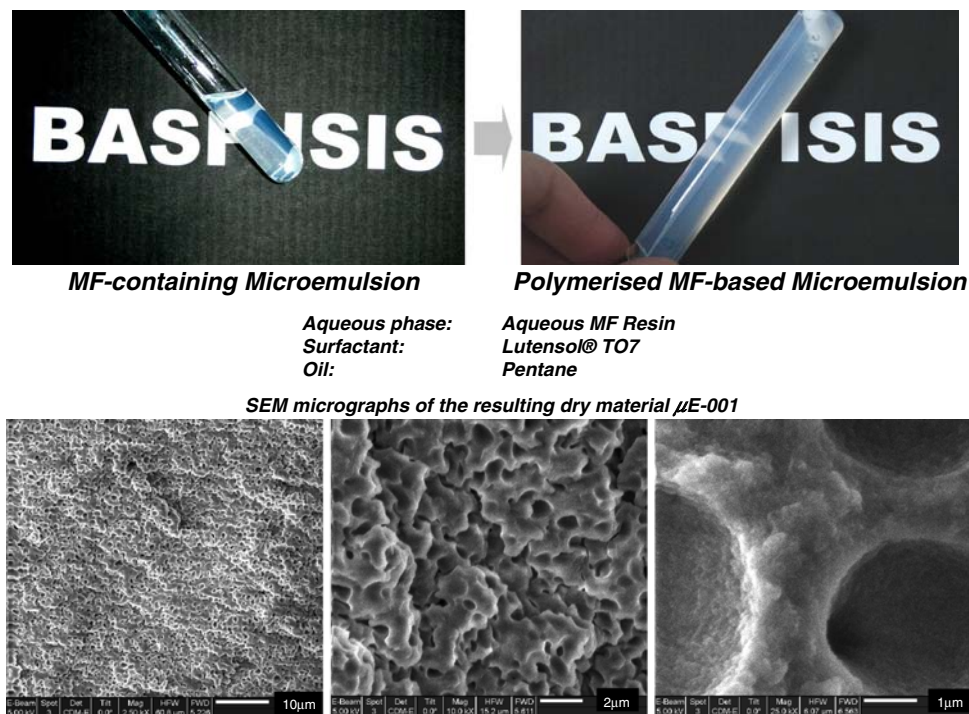

MF-containing Microemulsion   **Polymerised MF-based Microemulsion**

Aqueous phase:	*Aqueous MF Resin*
Surfactant:	*Lutensol® TO7*
Oil:	*Pentane*

SEM micrographs of the resulting dry material µE-001

Fig. 3 *Top Left*: Photographs of a bicontinuous microemulsion prepared with Lutensol® TO7 8.3 wt.%, heptane/water = 50% and a solution of MF as the aqueous phase (16.7 wt.% MF resin with M:F 1:3.6). The microemulsion is blue and homogeneous (bicontinuous and one-phase region). *Top right*: Photograph of the same microemulsion after the aqueous phase containing the MF resin has been polymerised by strong-acid catalysis (4.3 wt.% H$_3$PO$_4$). The microemulsion is now as a gel and does not flow anymore. *Bottom*: Scanning electron micrographs of the microemulsion after drying both the heptane and water off (µE-001), at 2.5k, 10k, 25k magnification from left to right. (Hg intrusion measurements give intrusion volume 5.0 mL/g, surface area 156 m^2/g, 89 vol.% pores, pore diameter 1.2 µm)

Fig. 4 Scanning electron micrographs and mercury intrusion data for two microemulsion-based materials μE-002 and μE-003 prepared with ionic surfactants and melamine formaldehyde resin under strong acid-catalysis (for synthesis detail of μE-002 and μE-003 refer to Table 2). μE-002 exhibits bimodal distribution of pore sizes with relatively higher intrusion volume and surface area whereas μE-003 contains only one average pore size, however with an overall low surface area
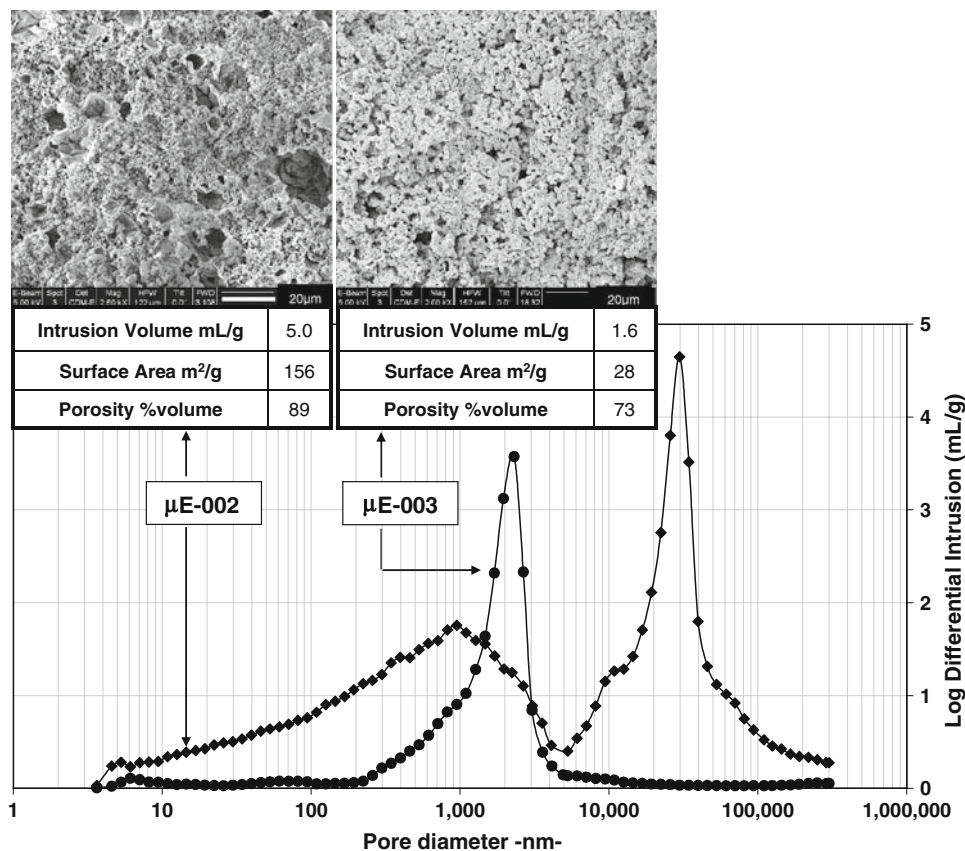
pentane is excluded. The SEM micrographs in Fig. 3 strongly suggest that under the given conditions the bicontinuous microemulsion evolves towards a macro-scopic O/W emulsion during polymerization. It is also important to recall that the structure of the initial micro-emulsion is characterized by a dynamic equilibrium of surface active species creating a system of zero curvature. Although the MF resin can be considered as partially sur-face active, the results clearly reveal that the microemulsion structure is strongly destabilized upon polymerisation of the MF species, irrespective of the surfactant type.

In an attempt to overcome the tendency of the system to give up its initial nanoscopic structure upon polymeriza-tion, the reaction parameters affecting the kinetics and phase separation were varied. Earlier investigations using microemulsion templating for the production of nanopor-ous materials through free radical polymerization failed [17, 18] except when applying ultrafast initiation e.g. gamma irradiation or macromers [19]. Indeed, it has been shown by Blank [20] that different catalysts can be used to cure MF-based resins: strong acids for fully alkylated MF resins and weak acids for amine-rich MF (either partially alkylated or not alkylated at all). The two catalysis mech-anisms differ and are referred to as specific acid-catalysis or general acid-catalysis, respectively. Although Reference [20] deals with curing of MF resins at very high resin

concentration rather than in a sol–gel environment as given here, the chemistry of the catalysis process remains the same and the same concepts of stabilising intermediate MF-based species could be applied. As a way to study the influence of the nature of the acid onto the polymerisation of MF in microemulsions systems, fresh bicontinuous microemulsions containing MF are prepared and then acid-catalysed using a weak acid instead (formic acid). Typi-cally materials such as μE-004 are formed after drying (see Fig. 5). MF aggregates are rather large and spherical and, based on scanning electron microscopy observations, do not form an interpenetrating three-dimensional structure of voids and MF. Pore size distribution from mercury poros-imetry reveal very large pores (2–10 μm) creating a pore volume of 80%. Despite numerous attempts using formic acid and varying parameters such as acid content, surfac-tant concentration, nature of surfactant (purely non-ionic or mixture non-ionic, anionic), it has not been possible to optimise and secure a stable bicontinuous structure upon acid-catalysis of MF.

This work clearly shows the difficulty in tackling a pore dimension over a few tens to hundreds of nanometers within highly porous polymeric networks. Indeed, the microemulsion templating approach has not yet proved successful in terms of pore size control which can be attributed to the fact that the present melamine

Fig. 5 Scanning electron micrograph and mercury intrusion data for one microemulsion-based material μE-004 prepared with an ionic surfactant and melamine formaldehyde resin under weak acid-catalysis (see synthesis detail in Table 2). μE-004 exhibits large porosity (80%) however with wide pores scattered between 1 to 10 microns in diameter
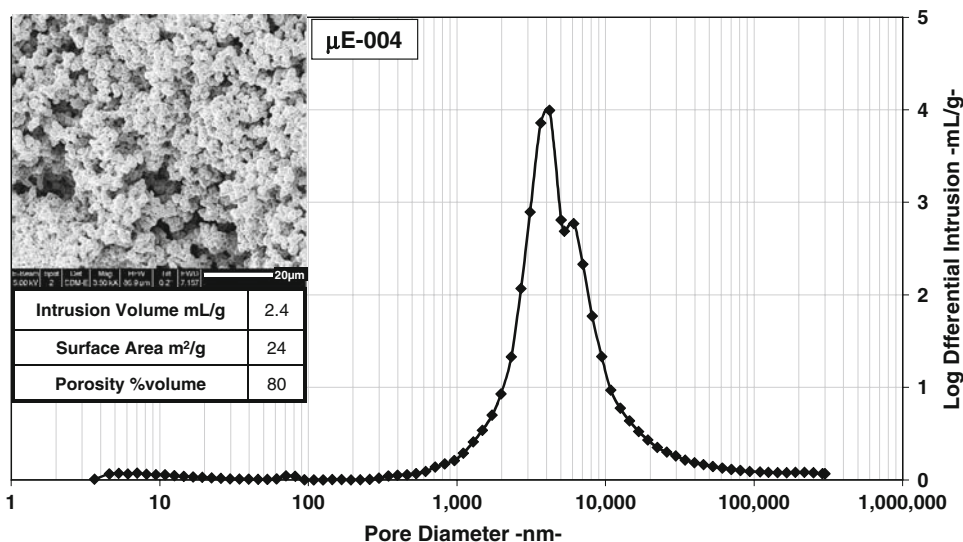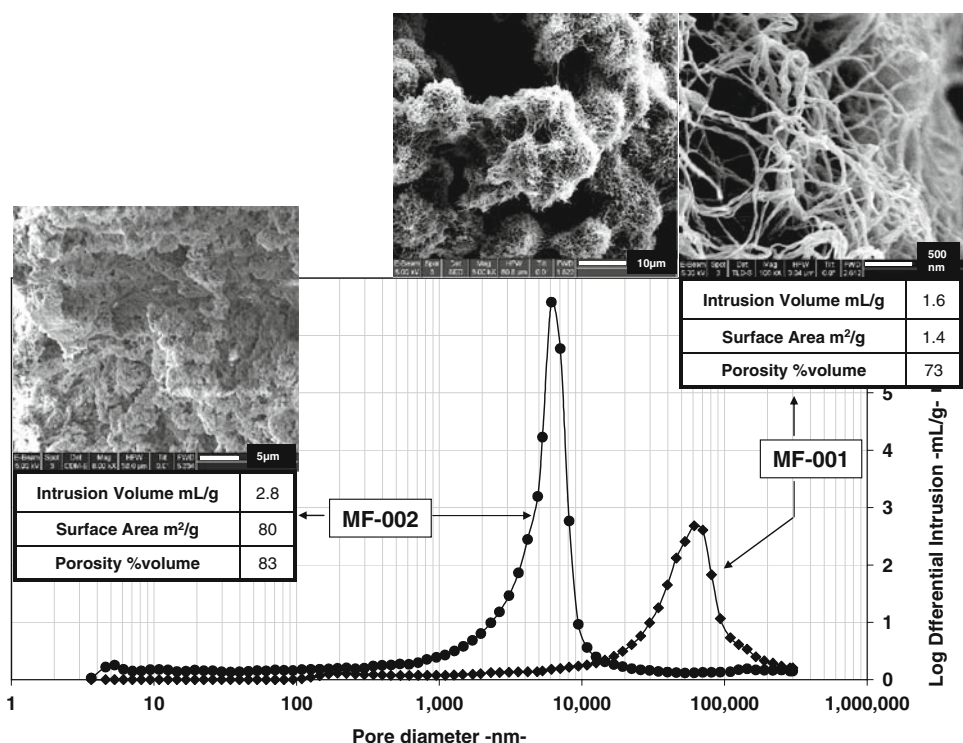

Intrusion Volume mL/g	2.4
Surface Area m²/g	24
Porosity %volume	80

Fig. 6 Scanning electron micrographs and mercury intrusion data of two materials MF-001 and MF-002 prepared with aqueous melamine-formaldehyde only, under strong and weak acid catalysis respectively. Using H_2SO_4 as the catalyst leads to fibre-like material MF001 with good porosity (73%) and low surface area (1.4 m²/g) whereas formic acid catalysed polymerisation of melamine formaldehyde results in particle like material with higher porosity and surface area (83% and 80 m²/g)

Intrusion Volume mL/g	1.6
Surface Area m²/g	1.4
Porosity %volume	73

Intrusion Volume mL/g	2.8
Surface Area m²/g	80
Porosity %volume	83

formaldehyde precondensate is not capable of stabilising the interface oil/aqueous phase during polymerisation. However, it is shown that the MF precondensate can be structured through the microemulsion in particular when non-ionic surfactants are used. Various surfactant head-groups have been tried as a means towards stabilising efficiently the oil/water interface. Only non-ionic surfactants either used solely or along with anionic surfactants have proved to be apparently able to retain the homogeneity in bicontinuous microemulsion systems at the early stages of polymerisation.

Phase separation could be arising from a thermodynamic loss of enthalpic or entropic free energy but also from a competing kinetic contribution due to the sol–gel process. In order to control the phase separation process, a few attempts were made by polymerising MF precondensates in water, without addition of surfactant and oil phase. Surprisingly some of the strong and multivalent acids give rise to a novel MF-based structure during sol–gel phase separation as demonstrated in Fig. 6. Therein, globules containing a strut-like interior structure is demonstrated for MF-001 obtained via sulphuric acid catalysis vs. MF002 as

obtained via formic acid catalysis. While the SEM micrograph of MF-002 represents a more common porous structure with MF globules resulting from phase separation during the sol–gel process, MF001 exhibits a remarkable thread-like morphology in the submicron scale. As suggested by the change in fractal structure from the micron to the nanometer range, it can be argued that the phase separation process is not induced by conventional nucleation of spherical particles upon polymerization. Instead, it can be suggested that this morphology stems from a specific interaction between the acid counterion (sulphate, carboxylate) with the slightly cationic amino resin. Note that the overall pore size distribution is shifted towards larger pores when compared with MF002, indicating that the ultrafine threads (as small as 50 nm in diameter) do not give rise to a large volume of pores in the 100 nm range. Current investigations aim at further elucidating the mechanism of acid controlled sol–gel morphology in organic porous materials.

4 Conclusion

The present work demonstrates a synthesis approach to design porous organic materials by using microemulsions as a structural template. Indeed, bicontinuous microemulsions are ideal candidates to template structures in the nanoscale due both to their 3D networks and dimensions but also to their thermodynamic stability. This study is the first attempt to carry out polycondensation reactions in the aqueous phase of bicontinuous microemulsions. Here the chosen monomers are water-soluble amino-resins (melamine formaldehyde MF). While many surfactants are not compatible with aqueous MF precondensates, we present a few single and mixed surfactant systems (ionic and non-ionic) that maintain the microemulsion nanostructure in the presence of the organic resin. Upon addition of the acid catalyst, however, the kinetics of polymerisation of the organic moiety competes with the stability of the template and a phase separation of the polymer from the aqueous phase is always observed at the microscopic level. Although no method was found to stabilise the oil–water interface during the polymerisation process, this work has however led to new experimental data which suggest that non-spherical MF morphologies (i.e. thread-like structures) can be obtained by specific interactions between the aqueous amino resin and the acid counterions.

References

1. Payra P, Dutta PK (2003) In: Auerbach SM, Carrado KA, Dutta PK (eds) Handbook of zeolite science and technology. Marcel-Dekker, NY
2. Cheetham AK, Ferey G, Loiseau T (1999) Angew Chem Int Ed 38(22):3268–3292
3. Singh R, Dutta PK (2003) In: Auerbach SM, Carrado KA, Dutta PK (eds) Handbook of zeolite science and technology. Marcel-Dekker, NY
4. Yanagisawa T, Shimizu T, Kuroda K, Kato C (1990) Bull Chem Soc Japan 63(4):988–992
5. Kresge CT, Leonowicz ME, Roth WJ, Vartuli JC, Beck JS (1992) Nature 359:710–712
6. Hüsing N, Schubert U (1998) Angew Chem Int Ed 37:22
7. Park CB, Baldwin DF, Suh NP (1995) Polym Eng Sci 35(5):432–440
8. Handa YP, Zhang Z, Wong B (2001) Cell Polym 20(1):1–16
9. Chen SH, Chang SL, Strey R, Samseth J, Mortensen K (1991) J Phys Chem 95(19):7427–7432
10. Sjiiblom J, Lindbergh R, Friberg SE (1996) Adv Colloid Interface Sci 95:125–287
11. Gan LM, Li TD, Chew CH, Teo WK (1995) Langmuir 11:3316–3320
12. Gan LM, Chieng TH, Chew CH, Ng SC (1994) Langmuir 10:4022–4026
13. Moulik SP, Paul BK (1998) Adv Colloid Interface Sci 78:99–195
14. Candau F, Pabon M, Anquetil J-Y (1999) Colloids Surf A 153:47–59
15. Sottmann T, Lade M, Stolz M, Schömacker R (2002) Tenside Surf Det 1:20–27
16. Egger CC, Schädler V, Hirschinger J, Raya J, Bechinger B (2007) Macromol Chem Phys 208(21):2204–2214
17. Antonietti M, Hentze H-P (1996) Colloid Polym Sci 274:696–702
18. Hentze H-P, Kaler E (2003) Curr Opin Colloid Interface Sci 8:164–178
19. Liu J, Gan LM, Chew CH, Teo WK, Gan LH (1997) Langmuir 13:6421–6426
20. Blank WJ (1979) J Coating Technol 51:61–70